Cerebral Cortex, 2017; 1–9

doi: 10.1093/cercor/bhx224
Original Article

ORIGINAL ARTICLE

Neuronal Migration and Axonal Pathways Linked to Human Fetal Insular Development Revealed by Diffusion MR Tractography

Avilash Das[1,2,3] and Emi Takahashi[2,3,4]

[1]Boston University School of Medicine, 72 E Concord St, Boston, MA, USA, [2]Division of Newborn Medicine, Department of Medicine, Boston Children's Hospital, Harvard Medical School, 1 Autumn St, Boston, MA, USA, [3]Fetal-Neonatal Brain Imaging and Developmental Science Center, Boston Children's Hospital, Harvard Medical School, 1 Autumn St, Boston, MA, USA and [4]Athinoula A. Martinos Center for Biomedical Imaging, Massachusetts General Hospital, Harvard Medical School, 149 13th St, Charlestown, MA, USA

Address correspondence to Emi Takahashi, Division of Newborn Medicine, Department of Medicine, Boston Children's Hospital, Harvard Medical School, 1 Autumn St. #453, Boston, MA 02115, USA. Email: emi@nmr.mgh.harvard.edu and Emi.Takahashi@childrens.harvard.edu

Abstract

The insula is a multimodal sensory integration structure that, in addition to serving as a gateway between somatosensory areas and limbic structures, plays a crucial role in autonomic nervous system function. While anatomical studies following the development of the insula have been conducted, currently, no studies have been published in human fetuses tracking the development of neuronal migration or of white matter tracts in the cortex. In this study, we aimed to follow the neuronal migration and subsequent maturation of axons in and around the insula in human fetal ages. Using high-angular resolution diffusion magnetic resonance imaging tractography, major white matter pathways to/from the insula and its surrounding operculum were identified at a number of time points during human gestation. Pathways likely linked to neuronal migration from the ventricular zone to the inferior frontal gyrus, superior temporal region, and the insular cortex were detected in the earliest gestational age studied (15 GW). Tractography reveals neuronal migration to areas surrounding the insula occurred at different time points. These results, in addition to demonstrating key time points for neuronal migration, suggest that neurons and axonal fiber pathways underlying the insula and its surrounding gyri mature differentially despite their relationship during cortical folding.

Key words: brain pathways, diffusion MRI, fetus, gyrus, human, insular cortex, tractography

Introduction

Anatomical studies tracking the growth of the insular cortex during gestation show that the insula is the first cortex to differentiate and develop beginning at 6 gestational weeks (GWs) in humans (Cunningham 1891; Retzius 1896; Streeter 1912; Kodama 1926; Benes 1994; Afif et al. 2007). The insula is a diverse region both functionally and connectively, with subregions involved in somatosensation, olfaction, interoception, motivation, and homeostatic function (Augustine 1996; Small et al. 1999; Craig 2002, 2009; Olausson et al. 2002; Shelly and Trimble 2004). The insula is known to have 3 predominate subdivisions, posterior, dorsal anterior, and ventral anterior (Chang et al. 2013; Borsook et al. 2016). The posterior subdivision, located near the auditory cortex and the SII region of the somatosensory cortex, has connectivity implicating it in both bodily sensations and interoception (Craig et al. 2000; Craig 2002; Olausson et al. 2002; Ostrowsky et al. 2002, Wager et al. 2004). The dorsal and the ventral anterior insula have associations in

emotion, chemo-sensation, and autonomic function (Pritchard et al. 1999; Chang et al. 2013; Gu et al. 2013; Borsook et al. 2016).

While many studies have been conducted examining connectivity of the insula in adults and adolescents (Angevine et al. 1962; Le Gros Clarkamd Russell 1939; Klinger and Gloor 1960; Yakovlev et al. 1960; Augustine 1996; Kalani et al. 2009; Cerliani et al. 2011; Cloutman et al. 2012; Dennis et al. 2014), few studies exist analyzing connectivity in newborns and during gestation; as a result, little is known about the development and time frame of insular maturation in fetuses. To better understand the development of the insular cortex, in this study, fetal human brains were examined using high-angular resolution diffusion MR imaging (HARDI) at multiple developmental time points through gestation to track the progression of neuronal migration to the insula, the superior temporal region (ST region), and the inferior frontal gyrus (IFG), as well as fiber development in those regions. The gyri surrounding the insula were included in order to observe the effect of neuronal migration during various stages of operculization.

Because white matter appears homogeneous in conventionally acquired structural magnetic resonance (MR) images, it is difficult to appreciate detailed pathways within the white matter with structural MR images. Alternative approaches employing tracer injections are limited to the study of a small number of white matter pathways in a localized area of the brain. HARDI tractography enables identification and discrimination of complex overlapping white matter pathways (Tuch et al. 2002; Berman et al. 2013), even in immature fetal brains (e.g., Takahashi et al. 2011, 2012), which are typically more challenging to segment due to a surplus of unmyelinated pathways. Although several techniques to assess white matter development have been established in addition to diffusion MR tractography (Ball et al. 2013; O'Muircheartaigh et al. 2014), diffusion tractography uniquely allows for the detection of 3-dimensional (3-D) pathways.

Neuronal precursor cells originating in the ventricle reach their ultimate cortical targets using radial glial scaffolding (Rakic 1972; Edmondson and Hatten 1987). While diffusion tractography traditionally has been used to detect white matter pathways, neuronal migration pathways are also visible (e.g., Takahashi et al. 2012; Xu et al. 2014). Radial tractography pathways from the ventricle can be often inferred to radial neuronal migration pathways (e.g., Takahashi et al. 2012). After migration is completed, radial glia retract and the migrated neurons differentiate in their target areas. Although it is not always obvious the difference between migration and axonal pathways using diffusion tractography, trajectories, and terminal regions of the pathways are the key to differentiate them (e.g., Wilkinson et al. 2016; Vasung et al. 2017). While gross anatomy studies following the development of the insular cortex have been conducted (Afif et al. 2007), currently, no studies have been published in human fetuses tracking the development of neuronal migration or white matter pathways in the insular cortex. In this work, we study the development of the insular cortex and its surrounding gyri (IF and ST gyri) in a series of human fetal ages using HARDI tractography with the intent to improve the current knowledge of the cortex and create a framework for future studies exploring normal and pathological development of the insula.

Materials and Methods

Fetal Brain Specimens

Eight brains were imaged for this study, with ages between 15 and 40 GWs. Postmortem brains were obtained from the Department of Pathology, Brigham, and Women's Hospital (BWH), Allen Institute Brain Bank (AIBB). Postmortem specimens were obtained with full parental consent. The primary cause of death was complications of prematurity. The brains were grossly normal, and standard autopsy examinations of all brains undergoing postmortem HARDI revealed minimal or no pathologic abnormalities at the macroscopic level. Images of vivo brains were obtained from Boston Children's Hospital (BCH). Living participants (1 newborn at 40 GW) had clinically indicated brain MRI studies that were diagnostically interpreted to show no abnormalities. Refer to Table 1 for summarized details on specimens. All research protocols were approved by the institutional review board.

Tissue Preparation for HARDI

At the time of autopsy, all brains were immersion fixed. The brains from BWH were stored in 4% paraformaldehyde, and the brains from AIBB were stored in 4% periodate-lysine-paraformaldehyde (PLP). During MR image acquisition, BWH brains were placed in Fomblin solution (Ausimont) (e.g., Takahashi et al. 2012) and AIBB brains were placed in 4% PLP. While these different solutions tend to change the background contrast (i.e., we see a dark background outside of the brain using Fomblin, and a bright background using PLP), these solutions do not specifically change diffusion properties (e.g., FA and ADC) within the brain parenchyma.

Diffusion MRI Procedures

Different scanner systems were used to accommodate different brain sizes (same as in e.g., Takahashi et al. 2012; Xu et al. 2014; Miyazaki et al. 2016; Wilkinson et al. 2016). MR coils that best fit each brain sample were used to ensure optimal imaging. The postmortem brain specimens from BWH were imaged with a 4.7 T Bruker Biospec MR system (specimens from 15 to 20, 26, and 31 GW), and specimens from the AIBB were imaged with a 3 T Siemens MR system (2 fetal specimens [21, 22 GW]) at the A. A. Martinos Center, Massachusetts General Hospital, Boston, MA, USA. The 3 T system was used to accommodate the AIBB brains that were in cranio and did not fit in the 4.7 T bore. To improve the imaging quality and obtain the best signal-to-noise ratio and high spatial resolution, we used custom-made MR coils with one channel on the 4.7 T and 3 T systems (Takahashi et al. 2012; Kolasinski et al. 2013; Xu et al. 2014).

For the BWH brains, a 3-D diffusion-weighted spin-echo echo-planar imaging (SE-EPI) sequence was used with a repetition time/echo time (TR/TE) of 1000/40 ms, with an imaging matrix of 112 × 112 × 112 pixels. Sixty diffusion-weighted

Table 1. Specimen-specific brain characteristics

Subject	Age	Source	Brain image
1	15 GW	BWH	Ex vivo
2	17 GW	BWH	Ex vivo
3	20 GW	BWH	Ex vivo
4	21 GW	AIBB	Ex vivo
5	22 GW	AIBB	Ex vivo
6	26 GW	BWH	Ex vivo
7	31 GW	BWH	Ex vivo
8	40 GW	BCH	In vivo

BWH, Brigham and Women's Hospital; AIBB, Allen Institute Brain Bank; BCH, Boston Children's Hospital.

measurements (with the strength of the diffusion weighting, $b = 8000\ s/mm^2$) and one nondiffusion-weighted measurement (no diffusion weighting or $b = 0\ s/mm^2$) were acquired with $\delta = 12.0$ ms and $\Delta = 24.2$ ms. The spatial resolution was $440 \times 500 \times 500$ μm. For the brains from the AIBB, diffusion-weighted data were acquired over 2 averages using a steady-state free-precession sequence with TR/TE = 24.82/18.76 ms, $\alpha = 60°$, and the spatial resolution was $400 \times 400 \times 400$ μm. Diffusion weighting was isotropically distributed along 44 directions ($b = 730\ s/mm^2$) with 4 $b = 0$ images. The in vivo sample (40 GW) from BCH was imaged on a 3 T Siemens MR system, Boston Children's Hospital, Boston, MA, USA. The diffusion pulse sequence used for imaging in vivo was a diffusion-weighted SE-EPI sequence, TR/TE 8320/88 ms, with an imaging matrix of $128 \times 128 \times 64$ pixels. The spatial resolution was $2 \times 2 \times 2$ mm. Thirty diffusion-weighted measurements ($b = 1000\ s/mm^2$) and 5 nondiffusion-weighted measurements ($b = 0\ s/mm^2$) were acquired with $\delta = 40$ ms and $\Delta = 68$ ms. We determined the highest spatial resolution for each brain specimen with an acceptable signal-to-noise ratio of more than 130 for tractography.

Reconstruction and Identification of Tractography Pathways

We used Diffusion Toolkit and TrackVis to reconstruct and visualize neural migration pathways. A streamline algorithm for diffusion tractography was used (Mori et al. 1999), described in previous publications (Schmahmann et al. 2007; D'Arceuil et al. 2008; Takahashi et al. 2010, 2011, 2012). The term "streamline" refers to connecting tractography pathways using a local maximum or maxima. This method is true for both DTI and HARDI. The streamline technique is limited in its ability to resolve crossing pathways when used with the traditional DTI technique because one simply connects the direction of the principal eigenvector on a tensor to produce the DTI tractography pathways. This feature is a recognized limitation of DTI (Mori et al. 1999). Hence, in the current study, we used HARDI, which can theoretically detect multiple local maxima on an orientation distribution function (ODF). Using each local maxima on an ODF, we applied the streamline algorithm to initiate and continue tractography (Tuch et al. 2003), thus enabling us to identify crossing pathways within a voxel.

Trajectories were propagated by consistently pursuing the orientation vector of least curvature. Tracking was terminated when the angle between 2 consecutive orientation vectors was greater than the given threshold (40°) or when the pathways extended outside of the brain surface using a brain mask. The brain mask volumes were used to terminate tractography structures instead of the FA threshold (Schmahmann et al. 2007; Wedeen et al. 2008; Takahashi et al. 2010, 2012; Vishwas et al. 2010), because progressive myelination and crossing pathways in the developing brain can result in low FA values and the use of an FA threshold may potentially incorrectly terminate tractography tracking in regions with low FA values.

Regions of interest

Hand-drawn regions of interest (ROI) were created along the ventricular walls in each specimen and were used as a start point for tracking migratory neurons to the insula and its surrounding gyri (Takahashi et al. 2012; Xu et al. 2014; Miyazaki et al. 2016). To track pathways between the insula and the edge of the ventricles, a second ROI was hand-drawn overlaying the insula and an ANY PART operator was used to detect pathways touching any part of the ROI. The same procedure was followed to track ventricular pathways in the IF and ST gyri. To track axonal fiber development, we used the previously made ROI overlays of the insular cortex, ST and IF gyri and tracked all pathways originating in the regions. Pathways that bowed away from the ventricles were selected by hand. U-shaped fiber development was tracked by placing an ROI sphere (diameter of 12 mm in 22 and 26 GW, 20 mm in 31 and 40 GW) in the meeting point between the parietal and temporal opercula and using a BOTH END restriction operator to select only U-fibers starting and ending within the ROI. We made sure all the U-fibers were included with the ROI, changing its size. In this study, only 1 hemisphere (right) was examined, as, for certain specimens, only one hemisphere of the brain was available. The color-coding of pathways is based on a standard RGB code, applied to the vector between the end-points of each fiber. Certain specimens (20 and 22 GW) were oriented differently during image acquisition, causing certain colorations of detected pathways to not match the other time points.

Results

IFG (Anterior to the Insula)

Tractography of the IFG, selecting for pathways originating/terminating in the ventricles, revealed a number of pathways between the ventricular and gyral surfaces. Pathways were detected from the earliest gestational age studied (15 GW). Figure 1*A–D* show these ventricle–IFG pathways at several stages between 15 and 21 GW, highlighting the consistent presence and prevalence of such pathways. By 21 GW, as shown in Figure 1*D,I*, some pathways appeared that do not originate/terminate in the ventricle (yellow arrows). This transition of fiber shape continued and was more prevalent in older gestational ages (Fig. 1*E–G*). By 22 GW, few ventricle–IFG pathways were present and most pathways had a clear separation from the ventricle (Fig. 1*E,H*, see orange arrows). Tractography at 26 GW showed no pathways between the ventricle and the gyral surface, with all pathways clearly separated from the ventricular surface (Fig. 1*F*). At 31 GW, the axonal fibers, seen in previous gestational ages, had a more dorsal/ventral trajectory and increased thickness, as compared with 26 GW. Additionally, a small population of ventricle–IFG pathways was once again seen (Fig. 1*G*, see pink arrow).

ST Gyrus (Posterior to the Insula)

Selecting for ventricular pathways in the ST region showed a small number of pathways between the ventricular and gyral surfaces at the earliest available gestational age (15 GW) (Fig. 2*A*). Similar ROI filtering in progressively older gestational ages (17–26 GW) showed a growing population of ventricle–ST pathways. Figure 2*B,C*, showing 17 and 20 GW respectively, show the same trajectories of pathways seen at 15 GW but with increased thickness. GWs 21 through 26 showed further increases in these pathways along the entirety of the ST region from a wider area of the ventricular surface (Fig. 2*D*–**F**, see red brackets). Tractography at 31 GW revealed a differential distribution of ventricular and cortical pathways (Fig. 3). Along the upper portion of the ST region, ventricle–ST pathways seen in previous gestational ages were fully replaced by cortical pathways (shown in red in the left-most panel and identified by the clear separation from the ventricle). In contrast, the lower portion of the ST gyrus is still primarily ventricle–ST pathways (shown in yellow in the left-most panel).

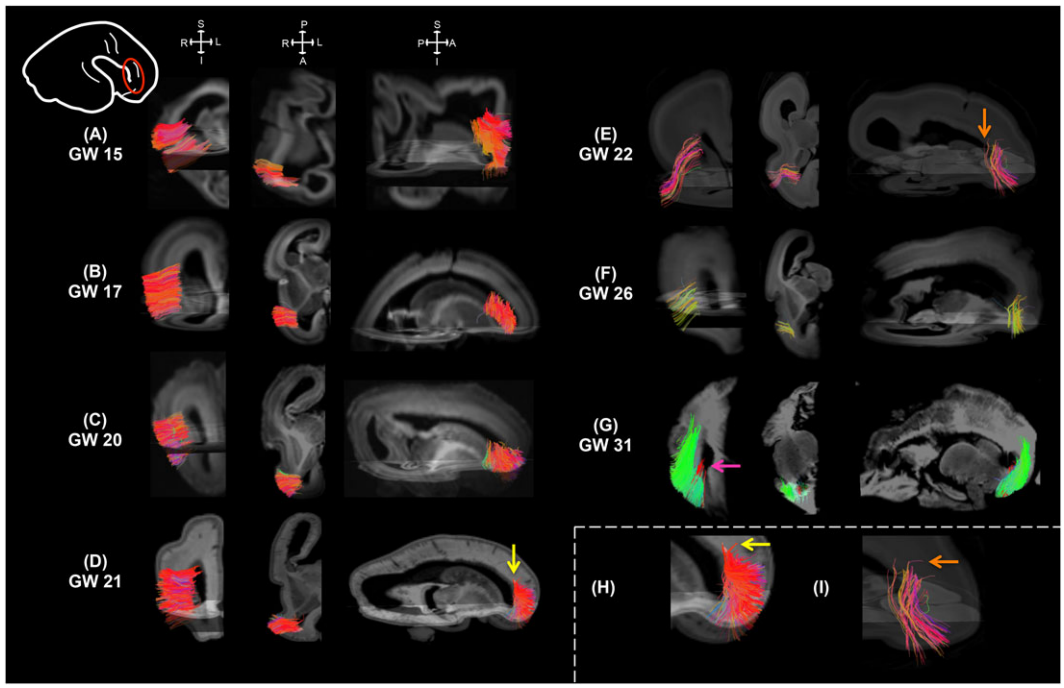

Figure 1. Coronal, transverse, and sagittal views showing radial migration and axonal pathways in the IFG in human GWs 15 through 31. In 31 GW, red pathways denote migratory pathways while green pathways are axonal. (*H*) and (*I*) show enlarged sagittal views of 21 and 22 GW respectively. Yellow arrows indicate first appearance of axonal pathways at 21 GW. Orange arrows at 22 GW indicate clearer separation of axonal pathways from the ventricle. Pink arrow indicates the reappearance of migratory ventricular pathways at 31 GW. Red circle in diagram indicates the ROI placement in the IF region. Diagram shown was hand-drawn from anatomical reference.

Insula

Tractography of the insular cortex revealed ventricular pathways primarily between the superior and anterior ventricular areas beneath the insula and the insular cortex. These ventricular-insular cortex pathways are present from the earliest available gestational age (15 GW) and are observed through 26 GW. Figure 4*A*,*B* (15 and 17 GW) show pathways between the edge of the ventricle and the insular cortex primarily in the superior and anterior ventricular surfaces. Pathways with distinct separation from the ventricle (seen in red in sagittal views) appeared in the posterior insular cortex (PIC) at 20 GW (Fig. 4*C*). Figure 4*D*–*F* show continued growth of these pathways from 21 to 26 GW. At 21 GW, the first of these cortical pathways were seen forming in the anterior insular cortex (AIC), while cortical pathways linked to the PIC further thicken; this observation continued through 26 GW, at which point ventricular-insular cortex pathways were sparse and had been largely replaced with cortical pathways in both the PIC and AIC. Tractography of the insular cortex at 31 GW showed only cortical pathways linked to the insular cortex, suggesting the completion of neuronal migration in this region (Fig. 4*G*). Further imaging of the insula at the time of birth (40 GW) showed the same basic connectivity as observed at 31 GW (Fig. 4*H*).

U-Shaped Short-Range Corticocortical Fibers

As the insula underwent opercularization, white matter pathways in the uppermost point of the parietal and temporal opercula were examined (see diagram of Fig. 5). U-shaped fiber formation connecting these 2 opercula began at 22 GW and was seen in every available gestational age following (Fig. 5). After the initial development, U-shaped fibers in this area did not expand noticeably along the length of the lateral sulcus until 40 GW. No other pathways likely linked to U- shaped fibers were found in either the insula or its surrounding opercula.

Discussion

In this study, we followed neuronal migration and subsequent maturation of axons in and around the insula in human fetal ages. These results, in addition to demonstrating key time points for neuronal migration, suggest that neurons and axonal pathways underlying the insula and its surrounding gyri mature differentially despite their relationship during cortical folding.

Inferior Frontal Gyrus

At the earliest gestational age, 15 GW, pathways were seen with end-points in both the IFG and the ventricular zone (VZ) (Fig. 1). The presence of these pathways in the VZ strongly suggests they are radial migration pathways (Rakic 1972) that originate in the VZ and terminate in the gyrus. Radial migratory pathways began to recede at 21 GW as indicated by the presence of preliminary axonal pathways that did not originate in the ventricle (Fig. 1*D*). The proliferation of axonal pathways and regression of migratory pathways continued until about 26 GW, at which point only axonal pathways were present (Fig. 1*F*). The time frame of this regression is consistent with previous studies studying radial migration in the fetal brain (Miyazaki et al. 2016).

At 31 GW axonal pathways were present in larger quantities than observed at 26 GW. This increased thickness of axonal pathways is likely associated with the continuing maturation of the frontal lobe. While neuronal migration to the IFG initially

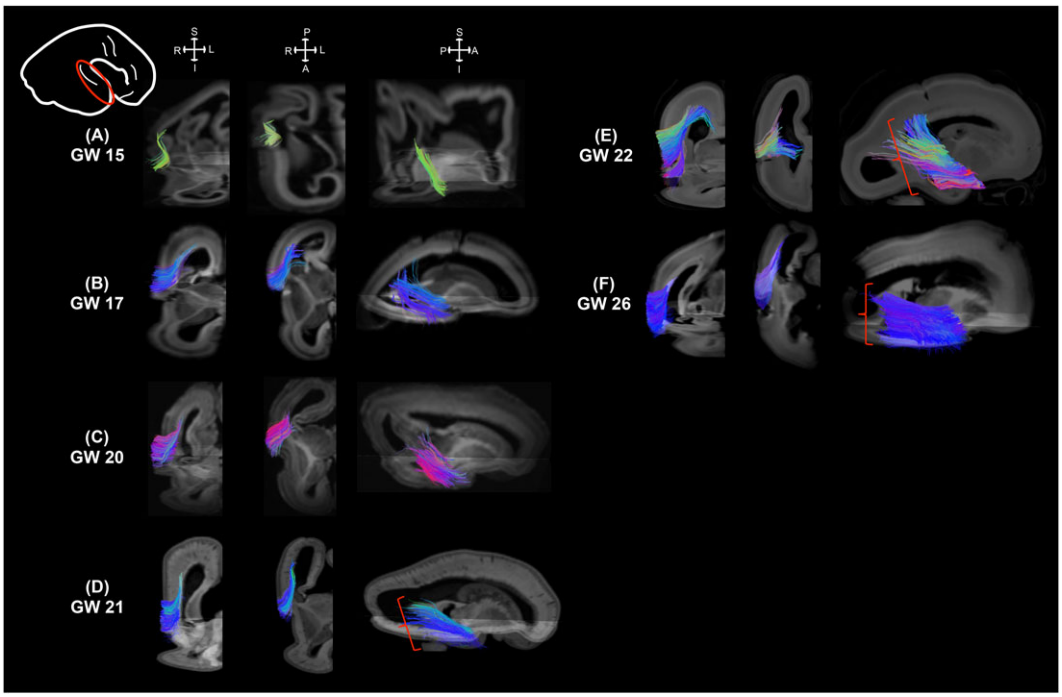

Figure 2. Coronal, transverse, and sagittal views showing radial migration pathways in ST gyrus in human GWs 15 through 26. Coloration differences in 20 and 22 GW are due to orientation of specimens during image acquisition. Red brackets indicate the increased spread of migration fibers from the ventricle between 21 and 26 GW. Red circle in diagram indicates the ROI placement in the ST region. Diagram shown was hand-drawn from anatomical reference.

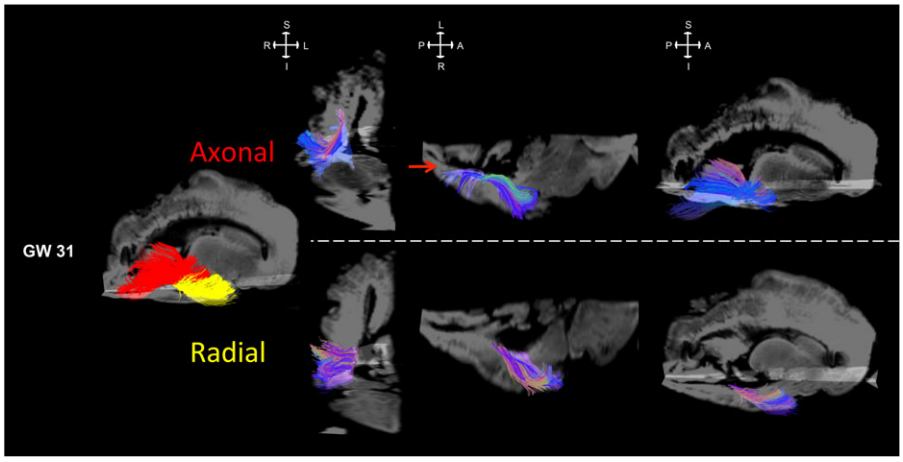

Figure 3. Coronal, transverse, and sagittal views showing radial migration and axonal pathways at 31 GWs. The multi-colored sagittal view shows a differential distribution of axonal and radial pathways. Axonal pathways are shown in red while radial pathways are shown in yellow. The red arrow indicates the axonal pathways' separation from the ventricle. The ROI placement in the figure is the same as seen in Figure 2.

concluded by 26 GW, a small population of radial pathways can be seen at 31 GW (Fig. 1G, shown in red). This appearance and disappearance of radial pathways may be a byproduct of the protracted growth of the frontal lobe. The radial migration fiber population seen in 31 GW likely represents a later round of neuronal migration (Gressens 2000; Paredes et al. 2016).

ST Gyrus

Based on the VZ–ST region connectivity, the pathways shown in Figure 2 are most likely radial migration pathways. At the earliest available gestational age, 15 GW, these migratory pathways were a small clustered population leading to the ST region from the upper posterior VZ, indicating radial migration to the ST region began near 15 GW. From 15 to 20 GW these radial pathways grew in number and thickened (Fig. 2A–C). Between 21 and 26 GW, radial pathways expanded, occupying a wider posterior ventricular surface, and reaching the lower ST region (Fig. 2D–F). This expansion and increasing neuron density of radial migration pathways appears consistent with previous studies conducted in primates (Cahalane et al. 2012; Charvet et al. 2015). While the appearance of axonal pathways and subsequent regression of radial pathways occurred near 21 GW in the IFG, in the ST gyrus, axonal pathways did not

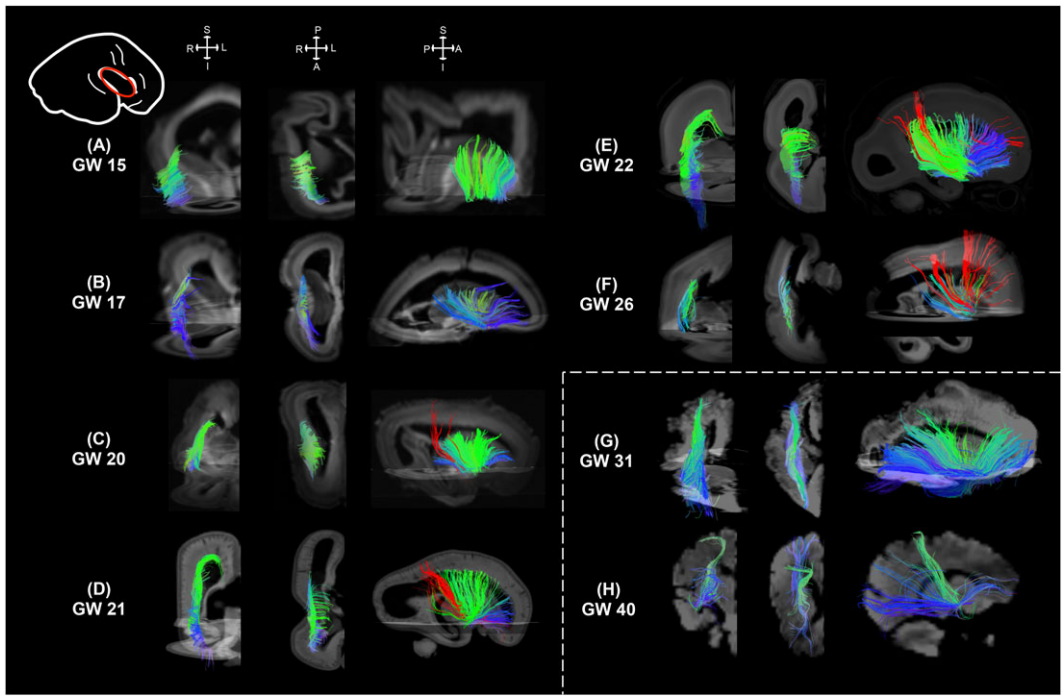

Figure 4. Coronal, transverse, and sagittal views showing radial migration and axonal pathways in the insular cortex in human GWs 15 through 40. In 15 through 26 GW red pathways indicate axonal pathways while all other pathways are migratory. Axonal pathways were only shown in sagittal views. All pathways shown in 31 and 40 GW are axonal. Red circle in diagram indicates the ROI placement in the insula. Diagram shown was hand-drawn from anatomical reference.

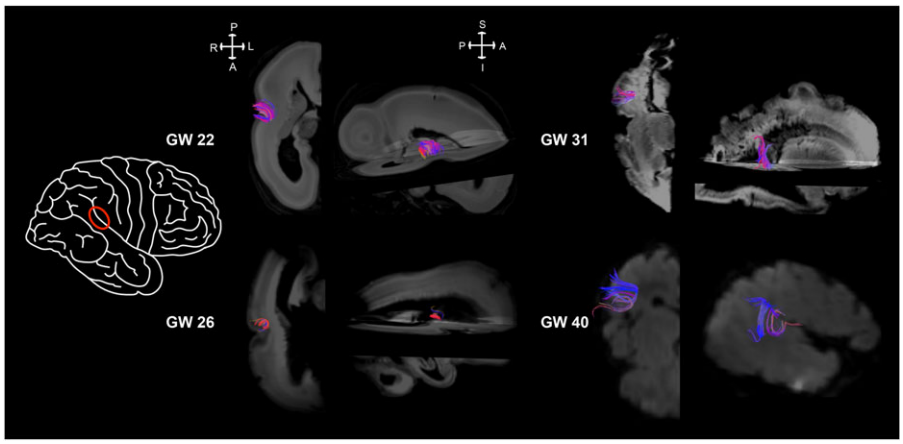

Figure 5. U-fiber development between the temporal and parietal opercula in 22 through 40 GWs. Red circle in diagram indicates the location of the U-fibers. Diagram shown was hand-drawn from anatomical reference.

begin developing until after 26 GW. This differential regression of axonal pathways is consistent with previous studies examining anterior–posterior asymmetry of migratory pathways (Miyazaki et al. 2016).

As seen in Figure 3, when axonal fiber development began between 26 and 31 GW it was primarily localized to the upper ST region while radial pathways were found along the lower gyrus. In earlier gestational ages radial pathways innervated the area that would later become the upper gyrus prior to spreading to the lower gyrus; therefore, it is possible this differential distribution of migratory and axonal pathways is due to the order in which neuronal migration pathways spread. Alternatively, the differential distribution may be a product of the different intended cell populations, as several lines of evidence have indicated the majority of radial migration pathways are implicated in the production of excitatory glutamatergic projection neurons (Rakic 1972, 1988; Bystron et al. 2008; Petanjek et al. 2009a, b). A future line of inquiry on this topic might, using histological methods, determine the distribution of neurons along the gyrus.

Insula

Directionally colored pathways in Figure 4 all appear to be radial migratory pathways due to their end-points in the VZ and the insula. Radial pathways to the insula were present and well structured from the earliest gestational age, indicating

neuronal migration to the area began several weeks prior to 15 GW. Pathways with a separation from the ventricle, most likely matured axonal pathways, initially began appearing in the PIC at 20 GW and successively in the AIC subdivisions at 21 GW (Fig 4C,D, see red pathways for axonal pathways). The PIC is known for connectivity implicating it in somatosensory recognition of pain, itch, and temperature (Damasio et al. 2000; Craig 2002, 2009; Harrison et al., 2010) while the AIC subdivisions are associated with higher-level functions such as emotion and awareness (Davidson and Irwin 1999; Kuo et al. 2009; Zaki et al. 2012). It is possible that matured axonal pathways first develop and thicken in the PIC due to its role in more basic bodily functioning as compared to the AIC and it is more cognitive role in higher-level processing.

By 26 GW, it is clear that the radial migration pathways in the insular region are regressing and the majority of pathways are axonal pathways. By 31 GW there are no pathways seen originating from the ventricles, indicating insular neuronal migration is fully completed. Tractography of the insula at 40 GW shows the same basic connectivity as seen in 31 GW demonstrating the lack of significant axonal fiber development following the termination of neuronal migration. Comparisons with insular connectivity studies in adults show many of the same pathways as witnessed in 40 GW (Cerliani et al. 2011; Cloutman et al. 2012), further highlighting the developmental importance of fetal insular development.

Gyral Development

In addition to examining the connectivity of the insula and its surrounding regions, at a number of time points during fetal development, we were able to gain insights into the gyrification process of the insular region. Van Essen's tension theory (1997) proposes mechanical forces necessary for cortical folding come from tension generated by axons pulling strongly interconnected cortical regions together. The theory specifically suggests that short-range inter-regional connections that traverse sulcal walls cause gyrification, and that sulci form between regions that are not so strongly connected. In both the ST and IF gyri, a distinct gyral structure had begun formation by 17 GW while operculization of the insula was underway by 20 GW. Between 17 and 20 GW, in both the ST region and the IFG, few, if any, pathways likely linked to axons were present, while most pathways detected were likely related to migratory pathways. These steps toward gyrification took place before or concurrently with the detection of the formation of axonal-like pathways in the gyri, suggesting that while axonal tension may play a role in shaping gyral structures, it likely does not play a major role in the initiation of gyrification. Alternative mechanisms, such as growth of large axons tracts (Goldman-Rakic and Rakic 1984), in late neurogenesis and even postnatally in some species (Ferrer et al. 1988; Sawada et al. 2012; Schmidt et al. 2012), and differential tangential expansion (Ronan et al. 2014) suggest multiple mechanisms may ultimately be responsible for gyrification. The results of this study, demonstrating the differential growth rate of different, related cortical regions, suggest differential tangential expansion has a significant role in the initiation of gyrification.

Limitations

The largest limitation of our study is the small number of specimens. It is difficult to resolve this issue, as securing large numbers of human fetal brain samples is difficult. The limited number of specimens available in this analysis (one per developmental stage) prevents us from concluding how well the crossing fibers are resolved per stage based on ODF maps and imposes substantial uncertainty to any reported quantitative findings and so we have relegated this topic to the future work.

To supplement the small sample size, we used brains from 2 different sources. Because brains from one of the sources (21 and 22 GW) had skulls, a different scanner system and scan parameters had to be used for them. Only 2 ex vivo specimens of 21 and 22 GW and 1 in vivo 40 GW subject were scanned at 3 T. For an in vivo subject, the 4.7 T small-bore scanner cannot be used, and the reason we used a 3 T scanner for the ex vivo brains was that they had skulls so did not fit into the 4.7 T scanner. At a 3 T scanner, high b values such as 8000 s/mm^2 is problematic to use because it makes significant artifacts with which tractography looks totally nonsense. We believe that the issue of different acquisition systems is not significant as tractography of both systems yielded similar trends. In Figure 1, the decrease in neuronal migration pathways was consistently observed in the IFG in 21 through 26 GW. Similarly, in Figure 4, a decrease in migratory fibers can be followed in the insula from 20 to 26 GW.

In addition to sample availability, the reliability of HARDI tractography must be acknowledged. The known pitfalls of the fiber reconstruction using HARDI have been reported in recent publication (Maier-Hein et al. 2016). In short, according to Maier-Hein et al., currently available algorithms for fiber pathway reconstruction tend to produce many false positive fibers, especially in periventricular regions (Maier-Hein et al. 2016). While our algorithms are similar to ones presented by Maier-Hein et al., we argue that, compared to the adult, the different architecture of fetal telencephalon, fewer number of established fiber crossings, and shorter fiber pathways lead to a significantly smaller number of reconstructed false positive pathways.

Funding

The Eunice Shriver Kennedy National Institute of Child Health and Human Development (NICHD) R01HD078561 and R21HD069001 (E.T.) and the National Institute of Neurological Disorders and Stroke (NINDS) R03NS091587 (E.T.). This study was conducted using postmortem human brain specimens from the tissue collection at the Department of Neurobiology at Yale University School of Medicine (supported by grant MH081896 from the National Institute of Mental Health), which form a part of the BrainSpan Consortium collection (http://www.brainspan.org). This research was carried out in part at the Athinoula A. Martinos Center for Biomedical Imaging at the Massachusetts General Hospital, using resources provided by the Center for Functional Neuroimaging Technologies, P41RR14075, a P41 Regional Resource supported by the Biomedical Technology Program of the National Center for Research Resources (NCRR), and the National Institutes of Health (NIH). This work also involved the use of instrumentation supported by the NCRR Shared Instrumentation Grant Program and/or High-End Instrumentation Grant Program; specifically grant number S10RR021110. The content of the manuscript is the view of the authors and does not necessarily represent the official views of the Eunice Shriver Kennedy NICHD, NINDS, or NIH. The data acquired in this study form a part of the BrainSpan Atlas of the Developing Human Brain. The BrainSpan data are accessible via the Allen Brain Atlas data portal http://www.brain-map.org or directly at http://www.developinghumanbrain.org or http://www.brainspan.org.

Notes

The other brain specimens were kindly provided by Dr Rebecca D. Folkerth, Brigham, and Women's Hospital, Boston Children's Hospital, and Harvard Medical School. We thank Dr. Lana Vasung for valuable comments on a previous version of this manuscript. *Conflict of interest*: None declared.

References

Afif A, Bouvier R, Buenerd A, Trouillas J, Mertens P. 2007. Development of the fetal insular cortex: study of the gyration from 13 to 28 gestational weeks. Brain Struct Funct. 212: 335–346.

Angevine JB, Locke S, Yakovlev PI. 1962. Limbic nuclei of thalamus and connections of limbic cortex. Arch Neurol. 7: 518–528.

Augustine JR. 1996. Circuitry and functional aspects of the insular lobe in primates including humans. Brain Res Rev. 22: 229–244.

Ball G, Boardman JP, Arichi T, Merchant N, Rueckert D, Edwards AD, Counsell SJ. 2013. Testing the sensitivity of tract-based spatial statistics to simulated treatment effects in preterm neonates. PLoS ONE. 8:e67706.

Benes FM. 1994. Development of the corticolimbic system. In: Dawson G, Fischer KW, editors. Human Behavior and the Developing Brain. New York: Guilford Press.

Berman JI, Lanza MR, Blaskey L, Edgar JC, Roberts TPL. 2013. High angular resolution diffusion imaging (HARDI) probabilistic tractography of the auditory radiation. Am J Neuroradiol. 34(8):1573–1578.

Borsook D, Veggeberg R, Erpelding N, Borra R, Linnman C, Burstein R, Becerra L. 2016. The Insula: A "Hub of Activity" in Migraine. Neuroscientist. 22(6):632–652.

Bystron I, Blakemore C, Rakic P. 2008. Development of the human cerebral cortex: Boulder Committee revisited. Nat Rev Neurosci. 9:110–122.

Cahalane DJ, Charvet CJ, Finlay BL. 2012. Systematic, balancing gradients in neuron density and number across the primate isocortex. Front.Neuroanat. 6:28.

Cerliani L, Thomas RM, Jbabdi S, Siero JCW, Nanetti L, Crippa A, Gazzola V, D'Arceuil H, Keysers C. 2011. Probabilistic tractography recovers a rostrocaudal trajectory of connectivity variability in the human insular cortex. Hum Brain Mapp. 33:2005–2034.

Chang LJ, Yarkoni T, Khaw MW, Sanfey AG. 2013. Decoding the role of the insula in human cognition: functional parcellation and large-scale reverse inference. Cereb Cortex. 23: 739–749.

Charvet CJ, Cahalane DJ, Finlay BL. 2015. Systematic, cross-cortex variation in neuron numbers in rodents and primates. Cereb Cortex. 25(1):147–160.

Cloutman LL, Binney RJ, Drakesmith M, Parker GJM, Lambon Ralph MA. 2012. The variation of function across the human insula mirrors its patterns of structural connectivity: evidence from in vivo probabilistic tractography. Neuroimage. 59:3514–3521.

Craig AD, Chen K, Bandy D, Reiman EM. 2000. Thermosensory activation of insular cortex. Nat Neurosci. 3(2):184–190.

Craig AD. 2002. How do you feel? Interoception: the sense of the physiological condition of the body. Nat Rev Neurosci. 3: 655–666.

Craig AD. 2009. How do you feel—now? The anterior insula and human awareness. Nat Rev Neurosci. 10:59–70.

Cunningham DJ. 1891. The development of the gyri and sulci on the surface of the island of Reil of the brain. J Anat Physiol. 25:338–348.

D'Arceuil H, Liu C, Levitt P, Thompson B, Kosofsky B, de Crespigny A. 2008. Three-dimensional high-resolution diffusion tensor imaging and tractography of the developing rabbit brain. Dev Neurosci. 30:262–275.

Damasio AR, Grabowski TJ, Bechara A, Damasio H, Ponto LL, Parvizi J, Hichwa RD. 2000. Subcortical and cortical brain activity during the feeling of self-generated emotions. Nat Neurosci. 3:1049–1056.

Davidson RJ, Irwin W. 1999. The functional neuroanatomy of emotion and affective style. Trends Cogn Sci. 3:11–21.

Dennis EL, Jahanshad N, McMahon KL, de Zubicaray GI, Martin NG, Hickie IB, Thompson PM. 2014. Development of insula connectivity between ages 12 and 30 revealed by high angular resolution diffusion imaging. Hum Brain Mapp. 35(4):1790–1800.

Edmondson JC, Hatten ME. 1987. Glial-guided granule neuron migration in vitro: a high resolution time-lapse video microscopic study. J Neurosci. 7:1928–1934.

Ferrer I, Hernåndez-Marti M, Bernet E, Galofré E. 1988. Formation and growth of the cerebral convolutions. I. Postnatal development of the median-suprasylvian gyrus and adjoining sulci in the cat. J Anat. 160:89–100.

Goldman-Rakic PS, Rakic P. 1984. Experimental modification of gyral patterns. In: Geschwind N, Galaburda A, editors. Cerebral dominance: biological foundations. Cambridge (MA): Harvard University Press. p. 179–192.

Gressens P. 2000. Mechanisms and disturbances of neuronal migration. Pediatr Res. 48(6):725–730.

Gu X, Liu X, Van Dam NT, Hof PR, Fan J. 2013. Cognition–emotion integration in the anterior insular cortex. Cereb Cortex. 23:20–27.

Harrison NA, Gray MA, Gianaros PJ, Critchley HD. 2010. The embodiment of emotional feelings in the brain. J Neurosci. 30:12878–12884.

Kalani MY, Kalani MA, Gwinn R, Keogh B, Tse VC. 2009. Embryological development of the human insula and its implications for the spread and resection of insular gliomas. Neurosurg Focus. 27(2):E2.

Klinger J, Gloor P. 1960. The connections of the amygdala and of the anterior temporal cortex in the human brain. J Comp Neurol. 115:333–369.

Kodama S. 1926. Über die sogenannten Basalganglien, Morphogenetische und pathologisch-anatomische Untersuchunger. Schweiz Arch Neurol Psychiatr. 18:179–246.

Kolasinski J, Takahashi E, Stevens AA, Benner T, Fischl B, Zöllei L, Grant PE. 2013. Radial and tangential neuronal migration pathways in the human fetal brain: anatomically distinct patterns of diffusion MRI coherence. Neuroimage. 1(79): 412–422.

Kuo WJ, Sjostrom T, Chen YP, Wang YH, Huang CY. 2009. Intuition and deliberation: two systems for strategizing in the brain. Science. 324:519–522.

Le Gros Clark WE, Russell WR. 1939. Observations on the efferent connexions of the centre median nucleus. J Anat. 73: 255–263.

Maier-Hein K, Neher P, Houde JC, Cote MA, Garyfallidis E, Zhong J, Chamberland M, Yeh FC, Lin YC, Ji Q, et al. 2016. Tractography-based connectomes are dominated by false-positive connections. bioRxiv, p.084137.

Miyazaki Y, Song JW, Takahashi E. 2016. Asymmetry of radial and symmetry of tangential neuronal migration pathways in developing human fetal brains. Front Neuroanat. 10:2.

Mori S, Crain BJ, Chacko VP, van Zijl PC. 1999. Three-dimensional tracking of axonal projections in the brain by magnetic resonance imaging. Ann Neurol. 45:265–269.

Olausson H, Lamarre Y, Backlund H, Morin C, Wallin BG, Starck G, Ekholm S, Strigo I, Worsley K, Vallbo ÅB, et al. 2002. Unmyelinated tactile afferents signal touch and project to insular cortex. Nat Neurosci. 5(9):900–904.

O'Muircheartaigh J, Dean DC III, Ginestet CE, Walker L, Waskiewicz N, Lehman K, Deoni SCL. 2014. White matter development and early cognition in babies and toddlers. Hum Brain Mapp. 35:4475–4487.

Ostrowsky K, Magnin M, Ryvlin P, Isnard J, Guenot M, Maugiére F. 2002. Representation of pain and somatic sensation in the human insula: a study of responses to direct electrical cortical stimulation. Cereb Cortex. 12:376–385.

Pritchard TC, Macaluso DA, Eslinger PJ. 1999. Taste perception in patients with insular cortex lesions. Behav Neurosci. 113: 663–671.

Paredes MF, James D, Gil-Perotin S, Kim H, Cotter JA, Ng C, Sandoval K, Rowitch DH, Xu D, McQuillen PS, et al. 2016. Extensive migration of young neurons into the infant human frontal lobe. Science. 354:aaf70731–7.

Petanjek Z, Berger B, Esclapez M. 2009a. Origins of cortical GABAergic neurons in the cynomolgus monkey. Cereb Cortex. 19:249–262.

Petanjek Z, Kostović I, Esclapez M. 2009b. Primate-specific origins and migration of cortical GABAergic neurons. Front Neuroanat. 3:26.

Rakic P. 1972. Mode of cell migration to the superficial layers of fetal monkey neocortex. J Comp Neurol. 145:61–83.

Rakic P. 1988. Specification of cerebral cortical areas. Science. 241(4862):170–176.

Retzius G. 1896. Das Menschenhirn; Studien in der makroskopischen Morphologie. Vol. 1. Norstedt: Stockholm.

Ronan L, Voets N, Rua C, Alexander-Bloch A, Hough M, Mackay C, Crow TJ, James A, Giedd JN, Fletcher PC. 2014. Differential tangential expansion as a mechanism for cortical gyrification. Cereb Cortex. 24(8):2219–2228. http://doi.org/10.1093/cercor/bht082.

Sawada K, Fukunishi K, Kashima M, Saito S, Sakata-Haga H, Aoki I, Fukui Y. 2012. Fetal gyrification in cynomologus monkeys: a concept of developmental stages in gyrification. Anat Rec. 295:1065–1074.

Schmahmann JD, Pandya DN, Wang R, Dai G, D'Arceuil HE, de Crespigny AJ, Wedeen VJ. 2007. Association fibre pathways of the brain: parallel observations from diffusion spectrum imaging and autoradiography. Brain. 130:630–653.

Schmidt MJ, Amort K, Kramer M. 2012. Postnatal development of the cerebral gyrification in the canine brain. Vet Radiol Ultrasound. 53:643–649.

Shelley BP, Trimble MR. 2004. The insular lobe of Reil–its anatamico-functional, behavioural and neuropsychiatric attributes in humans—a review. World J Biol Psychiatry. 5: 176–200.

Small DM, Zald DH, Jones-Gotman M, Zatorre RJ, Pardo JV, Frey S, Petrides M. 1999. Human cortical gustatory areas: a review of functional neuroimaging data. Neuroreport. 10:7–14.

Streeter GL. 1912. Chapter XIV the development of the nervous system. In: Keibel F, Mall FP, editors. Manual of human embryology. Vol. II. Philadelphia: Lippincott.

Takahashi E, Dai G, Wang R, Ohki K, Rosen GD, Galaburda AM, Grant PE, Wedeen VJ. 2010. Development of cerebral pathways in cats revealed by diffusion spectrum imaging. NeuroImage. 49:1231–1240.

Takahashi E, Dai G, Rosen GD, Wang R, Ohki K, Folkerth RD, Grant EP. 2011. Developing neocortex organization and connectivity in cats revealed by direct correlation of diffusion tractography and histology. Cereb Cortex. 21:200–211.

Takahashi E, Folkerth RD, Galaburda AM, Grant PE. 2012. Emerging cerebral connectivity in the human fetal brain: An MR tractography study. Cereb Cortex. 2:455–464.

Tuch DS, Reese TG, Wiegell MR, Wedeen VJ. 2003. Diffusion MRI of complex neural architecture. Neuron. 40:885–895.

Tuch DS, Reese TG, Wiegell MR, Makris N, Belliveau JW, Van Wedeen J. 2002. High angular resolution diffusion imaging reveals intravoxel white matter fiber heterogeneity. Magn Res Med. 48:577–582.

Van Essen DC. 1997. A tension-based theory of morphogenesis and compact wiring in the central nervous system. Nature. 385:313–318.

Vasung L, Raguz M, Kostovic I, Takahashi E. 2017. Spatiotemporal relationship of brain pathways during human fetal development using high-angular resolution diffusion MR imaging and histology. Front Neurosci. 11:348.

Vishwas MS, Chitnis T, Pienaar R, Healy BC, Grant PE. 2010. Tract-based analysis of callosal, projection, and association pathways in pediatric patients with multiple sclerosis: a preliminary study. AJNR Am J Neuroradiol. 31:121–128.

Wager TD, Rilling JK, Smith EE, Sokolik A, Casey KL, Davidson RJ, Kosslyn SM, Rose RM, Cohen JD. 2004. Placebo-induced changes in FMRI in the anticipation and experience of pain. Science. 303:1162–1167.

Wedeen VJ, Wang RP, Schmahmann JD, Benner T, Tseng WYI, Dai G, Pandya DN, Hagmann P, D'Arceuil H, de Crespigny AJ. 2008. Diffusion spectrum magnetic resonance imaging (DSI) tractography of crossing fibers. Neuroimage. 41:1267–1277.

Wilkinson M, Kane T, Wang R, Takahashi E. 2016. Migration pathways of thalamic neurons and development of thalamocortical connections in humans revealed by diffusion MR tractography. Cereb Cortex. doi:10.1093/cercor/bhw339[Epub ahead of print].

Xu G, Takahashi E, Folkerth RD, Haynes RL, Volpe JJ, Grant PE, Kinney HC. 2014. Radial coherence of diffusion tractography in the cerebral white matter of the human fetus: neuroanatomic insights. Cereb Cortex. 24:579–592.

Yakovlev PI, Locke S, Koskoff DY, Patton RA. 1960. Limbic nuclei of the thalamus and connections of the limbic cortex. I. Organization of the projections of the anterior group of nuclei and of the midline nuclei of the thalamus to the anterior cingulate gyrus and hippocampal rudiment in the monkey. Arch Neurol. 3:620–641.

Zaki J, Davis JI, Ochsner KN. 2012. Overlapping activity in anterior insula during interoception and emotional experience. Neuroimage. 62:493–499.